Cobalt enrichment in anaerobic microbial cocultures revealed by synchrotron X-ray fluorescence imaging

Jennifer B. Glass[1*] *Si Chen*[2], *Katherine S. Dawson*[3], *Damian R. Horton*[1], *Stefan Vogt*[2], *Ellery D. Ingall*[1], *Benjamin S. Twining*[4], *Victoria J. Orphan*[3]

[1]School of Earth and Atmospheric Sciences, Georgia Institute of Technology, Atlanta, Georgia USA;

[2]Advanced Photon Source, Argonne National Laboratory, Argonne, Illinois, USA;

[3]Division of Geological and Planetary Sciences, California Institute of Technology, Pasadena, California, USA;

[4]Bigelow Laboratory for Ocean Sciences, East Boothbay, Maine, 04544, USA;

Keywords: methanogen, sulfate reduction, cobalt, methanol, synchrotron x-ray fluorescence

Running Head: Cobalt enrichment in cocultures

***Corresponding Author:** Jennifer.Glass@eas.gatech.edu

Abstract

This study examined iron, cobalt, nickel, copper, and zinc content of a model sulfate-reducing bacterium and methanogenic archaeon in mono- vs. coculture. Inductively coupled plasma mass spectrometry and synchrotron x-ray fluorescence microscopy were used to compare elemental content of bulk vs. single cells. Cocultures contained more cellular cobalt than monocultures as well as distinct nanoparticulate zinc- and cobalt/copper- sulfides. This study provides the first evidence that microbes have different metal quotas in mono- vs. coculture, and that cocultures grown in micromolar metal concentrations precipitate different metal sulfide minerals than previous studies of sulfate-reducing bacteria grown at millimolar metal concentrations.

Introduction

In anoxic natural and engineered environments, sulfate-reducing bacteria and methanogenic archaea perform the last two steps of organic carbon respiration, releasing chemically reactive sulfide and climatically active methane. Sulfate-reducing bacteria and methanogenic archaea can exhibit cooperative or competitive interactions depending on sulfate and electron donor availability (Brileya et al. 2014; Bryant et al. 1977; Ozuolmez et al. 2015; Stams and Plugge 2009). In the presence of methanol, an major industrial substrate, sulfate reduction and methanogenesis occur simultaneously in cocultures (Dawson et al. 2015; Phelps et al. 1985), anoxic sediments (Finke et al. 2007; Oremland and Polcin 1982), and anaerobic digesters (Spanjers et al. 2002; Weijma and Stams 2001).

Metalloenzymes are essential for both sulfate reduction and methylotrophic methanogenesis (Barton et al. 2007; Ferry 2010; Glass and Orphan 2012; Thauer et al. 2010). Iron is needed for cytochromes and iron-sulfur proteins in both sulfate-reducing bacteria (Fauque and Barton 2012; Pereira et al. 2011) and methylotrophic methanogens (Thauer et al. 2008).

Cobalt and zinc are present in the first enzymes in sulfate reduction (ATP sulfurylase, Sat; Gavel et al. 1998; Gavel et al. 2008), and methylotrophic methanogenesis (methanol:coenzyme M methyltransferase; Hagemeier et al. 2006). Nickel is found in the final enzyme in methanogenesis (methyl coenzyme M reductase; Ermler et al. 1997), and zinc is present in the heterodisulfide reductase that recycles cofactors for the methyl coenzyme M reductase enzyme (Hamann et al. 2007). Nickel and cobalt are required by methanogenic archaea and sulfate-reducing bacteria that are capable of complete organic carbon oxidization for carbon monoxide dehydrogenase/acetyl Co-A synthase in the Wood-Ljungdahl CO_2 fixation pathway (Berg 2011; Ragsdale and Kumar 1996). Hydrogenases containing Ni and Fe are functional in many, but not all, sulfate-reducing bacteria (Osburn et al. 2016; Pereira et al. 2011) and methylotrophic methanogens (Guss et al. 2009; Thauer et al. 2010). Evidence for high metabolic metal demands is provided by limited growth of methanogenic archaea without Co and Ni supplementation in methanol-fed monocultures (Scherer and Sahm 1981) and anaerobic bioreactors (Florencio et al. 1994; Gonzalez-Gil et al. 1999; Paulo et al. 2004; Zandvoort et al. 2003; Zandvoort et al. 2006).

Sulfate-reducing bacteria produce sulfide, which can remove toxic metals from contaminated groundwater due to precipitation of metal sulfides with low solubility (Paulo et al. 2015). Metal sulfides may also limit the availability of essential trace metals for microbial metabolism (Glass and Orphan 2012; Glass et al. 2014). Numerous studies have investigated the effect of heavy metals on anaerobic metabolisms at millimolar concentrations in heavy-metal contaminated industrial wastewaters, whereas few studies have investigated interactions between anaerobic microbes and transition metals at the low micro- to nanomolar metal concentrations present in most natural ecosystems and municipal wastewaters (see Paulo et al. 2015 for review).

Due to the importance of trace metals for anaerobic microbial metabolisms in bioremediation and wastewater treatment, extensive efforts have focused on optimizing metal concentrations to promote microbial organic degradation in anaerobic digesters (for review, see Demirel and Scherer (2011)). However, studies of the metal content of anaerobic microbes have almost solely employed non-spatially resolved techniques such as ICP-MS on monocultures (Barton et al. 2007; Cvetkovic et al. 2010). Thus, application of previous data to complex microbial communities is limited, with few exceptions (Neveu et al. 2016; Neveu et al. 2014). In this study, we tested the hypothesis that methanogenic archaea and sulfate-reducing bacteria possess different cellular elemental contents when grown in monocultures vs. coculture. *Methanosarcina acetivorans* C2A, a well-studied strain capable of growing via aceticlastic and methylotrophic methanogenesis, but not on H_2/CO_2, was chosen as the model methanogenic archaeon. For the model sulfate-reducing bacterium, we chose the metabolically versatile species *Desulfococcus multivorans*, which is capable of complete organic carbon oxidation. Individual cells of mono- and cocultures of these two species were imaged for elemental content on the Bionanoprobe (Chen et al. 2013) at the Advanced Photon Source (Argonne National Laboratory) and compared to bulk cellular metal contents measured by ICP-MS.

Materials and Methods

Culture growth conditions

Monocultures of *Methanosarcina acetivorans* strain C2A (DSM 2834) and *Desulfococcus multivorans* (DSM 2059) were grown with 60 mM methanol and 20 mM lactate, respectively, as described in Dawson et al. (2015). Cocultures were inoculated into sterile media containing 60 mM methanol and 20 mM lactate to equal initial cell densities of the two species. After 12 days

of growth, mono- and cocultures were frozen and pelleted for ICP-MS analysis, or prepared for SXRF imaging.

ICP-MS

Frozen cell pellets were dried in acid-washed Savillex Teflon vials in an exhausted laminar flow hood, yielding 5-20 mg dry weight per sample. Cells were digested overnight at 150°C in 2 mL of trace metal grade nitric acid and 200 µL hydrogen peroxide, dried again, and dissolved in 5 mL 5% nitric acid. The medium was diluted 1:50 in nitric acid. The elemental content of microbial cells and media was analyzed by ICP-MS (Element-2, U Maine Climate Change Institute). Sterile medium contained the following concentrations (in µM): P, 800; Zn, 7; Fe, 4; Co, 2; Ni, 0.9; Cu, 0.3. Digestion acid blanks contained (in nM): P, 127; Zn, 12; Fe, 5; Co, 0.007; Ni, 0.9; Mo, 0.02; Cu, 0.1; V, 0.03.

SXRF sample preparation

Monocultures were prepared for SXRF analysis without chemical fixation by spotting onto silicon nitride wafers (Silson Ltd., cat. 11107126) followed by rinsing with 10 mM HEPES buffer, pH 7.8. Cocultures (500 µL) were incubated on ice for 1 hour in 50 mM HEPES and 0.6 M NaCl at pH 7.2 containing 3.8% paraformaldehyde and 0.1% glutaraldehyde cleaned of potential trace-metal contaminants with cation exchange resin (Dowex 50-W X8) following established protocols (Price et al. 1988; Twining et al. 2003). Cells were then centrifuged, re-suspended in 10 mM HEPES buffer, pH 7.8, and either embedded in resin and thin sectioned following the methods described in McGlynn et al. (2015) or spotted directly onto silicon nitride wafers.

SXRF analyses

SXRF analyses were performed at the Bionanoprobe (beamline 21-ID-D, Advanced Photon Source, Argonne National Laboratory). Silicon nitride wafers were mounted perpendicular to the beam as described in Chen et al. (2013). SXRF mapping was performed with monochromatic 10 keV hard X-rays focused to a spot size of ~100 nm using Fresnel zone plates. Concentrations and distributions of all elements from P to Zn were analyzed in fine scans using a step size of 100 nm and a dwell time of 150 ms. An X-ray fluorescence thin film (AXO DRESDEN, RF8-200-S2453) was measured with the same beamline setup as a reference. MAPS software was used for per-pixel spectrum fitting and elemental content quantification (Vogt 2003). Sample elemental contents were computed by comparing fluorescence measurements with a calibration curve derived from the measurements of the reference thin film. Regions of interest (ROIs) were selected with MAPS software by highlighting each microbial cell (identified based on elevated P content) or particle (identified based on elevated metal content). For each whole cell ROI (n=14 and n=18 for *D. multivorans* and *M. acetivorans* monocultures, respectively, and n=13 for the coculture), mean area-normalized and background-corrected elemental content in μg cm^{-2} was multiplied by cellular area to obtain molar elemental content per cell (mol $cell^{-1}$). Background corrections were performed by subtracting the mean of triplicate measurements of the elemental content for "blank" ROIs bordering the analyzed cells to account for the elemental content originating from each section of the SiN grid on which the cells were spotted. For thin sections, co-localization of three elements was performed with MAPS software. Statistical analysis was performed with JMP Pro (v. 12.1.0) using the Tukey-Kramer HSD test.

Fluorescence in situ hybridization

Fluorescence in situ hybridization was performed on separate aliquots from the same time point of the cell culture used for SXRF analyses. One mL of cell culture was preserved in 3%

paraformaldehyde for 1-3 hours, then washed and resuspended in 200 µL of 3x PBS:ethanol as described in Dawson et al. (2012). Four microliters of fixed cells were spotted onto a slide and hybridized with an oligonucleotide probe targeting *Methanosarcina acetivorans* MSMX860 (Raskin et al. 1994) and the deltaproteobacterial probe Delta495a (Loy et al. 2002)+ cDelta495a (Macalady et al. 2006). The FISH hybridization buffer contained 45% formamide, and the hybridization was carried out at 46°C for 2 hours followed by a 15 minute wash in 48°C washing buffer (Daims et al. 2005). The slides were rinsed briefly in distilled water, and mounted in a solution of DAPI (5 µg/mL) in Citifluor AF-1 (Electron Microscopy Services). Imaging was performed with a 100x oil immersion objective (Olympus PlanApo). Attempts to image cells by fluorescence microscopy after SXRF analysis were unsuccessful due to x-ray radiation damage.

Results

Cellular elemental content of monocultures

Cellular S contents were significantly higher in methanol-growth *M. acetivorans* (n=14) than lactate-grown *D. multivorans* (n=18; $p<0.0001$; Fig. 1; Table 1). Mean cellular P contents were 3 times higher in *M. acetivorans* than *D. multivorans*, but the difference was only significant at $p = 0.07$. Cellular metal contents followed the trend Fe ≫ Zn > Cu > Co > Ni and were not statistically different between the two species.

SXRF and ICP-MS comparison

Metal:P ratios from SXRF and ICP-MS data were compared for each monoculture (Table 2). For both techniques, the same trends were observed in metal:P ratios as for cellular metal content by SXRF (Fe ≫ Zn > Cu > Co > Ni). For each monoculture, metal:P ratios measured by the two methods were generally the same order of magnitude, but SXRF produced higher metal:P ratios

for the more abundant metals (Zn, Fe, and Cu), whereas ICP-MS yielded higher metal:P ratios for the less abundant metals (Co and Ni).

Relative abundance of species in coculture

Coculturing of both species for 12 days in media containing methanol and lactate resulted in dominance of *M. acetivorans* (77%, or 1,753 cells hybridized with the MSMX860 FISH probe) over *D. multivorans* (23%, or 522 cells hybridized with the Delta495a FISH probe) for 2,275 total cells counted in ten 100x (125 x 125 μm) fields of view. Cells were ~1 μm^2 cocci. No other cells stained with DAPI other than those that hybridized with MSMX860 and Delta495a oligonucleotide probes.

Cellular elemental content of cocultures

ICP-MS measurement of digested cocultured cells showed Co:P and Cu:P ratios 12-14% greater than predicted based on a 77% *M. acetivorans* and 23% *D. multivorans* mix of monocultures (Table 2), whereas Fe:P and Ni:P ratios were 20-30% lower than predicted, and the Zn:P ratio was the same as predicted. ICP-MS metal:P ratios for cocultures were 6-20 times higher than SXRF metal:P ratios.

Whole-cell SXRF imaging was performed on three grid areas containing 30, 15, and 3 total cells. ROI areas were 13 cocultured cells were quantified in this dataset, with care taken to avoid regions of elevated non-cellular metals (see Fig. 2 and next section). No visual difference in elemental distribution was observed between cells (Fig. 2). Cellular P content was significantly higher in the cocultured cells than in monocultures ($p<0.0001$; Table 1). Cellular S content of cocultured cells was statistically indistinguishable from the *D. multivorans* monoculture and significantly lower than the *M. acetivorans* monoculture ($p<0.0001$; Fig. 1). Cocultured cells contained significantly higher Co and Ni than monocultured cells ($p<0.0001$;

Fig 1). Coculture Fe and Zn contents fell in the same range as monocultures, while cellular Cu contents were significantly lower in cocultures than monocultures ($p<0.05$).

Non-cellular metals in cocultures

In whole cell SXRF images, discrete non-cellular (low-P) hot spots of Zn (max: 0.7 μg cm^{-2}), Co (max: 0.4 μg cm^{-2}) and S (max: 2.7 μg cm^{-2}) were present amongst a cluster of cocultured cells identified as P-rich cocci (Fig. 2). In thin sections, semi-circular non-cellular Zn hot spots (0.6 ± 0.1 μm^2; n=8) containing ~1:1 molar ratios of Zn:S (17 ± 2 μg Zn cm^{-2}: 7.6 ± 0.7 μg S cm^{-2}) were interspersed amongst cell clusters (Fig. 3a-e). The Zn hot spots were spatially segregated from more numerous semi-circular non-cellular cobalt globules of the same size (0.6 ± 0.1 μm^2; n=45) containing 2.1 ± 0.1 μg Co cm^{-2}, 3.4 ± 0.2 μg S cm^{-2}, and 1.3 ± 0.1 μg Cu cm^{-2}. Discrete semi-circular patches of elevated Ni (max: 2.9 μg cm^{-2}) with low S content were observed in two imaging fields (Fig. 3b,c).

Discussion

In this study, SXRF enabled imaging and quantification of trace metals in cellular and abiotic phases at the single-cell scale. The range of cellular metal quotas (10^{-16} to 10^{-20} mol $cell^{-1}$) reported here for the sulfate-reducing bacterium *Desulfococcus multivorans* and methanogenic archaeon *Methanosarcina acetivorans* based on SXRF is consistent with hyperthermophilic archaea measured by ICP-MS (10^{-17} to 10^{-20} g $cell^{-1}$, or 10^{-18} to 10^{-22} mol $cell^{-1}$, for first row transition metals (Cameron et al. 2012)). Moreover, our observation that Fe and Zn were the two most abundant cellular trace metals in monocultures is consistent with previous studies of diverse prokaryotes (Barton et al. 2007; Cvetkovic et al. 2010; Outten and O'Halloran 2001; Rouf 1964), including methanogens (Cameron et al. 2012; Scherer et al. 1983). To our knowledge, there are no previous reports of trace metal content of sulfate-reducing bacteria, but

196 the abundance of Fe and Zn-containing proteins encoded by their genomes (Barton and Fauque
197 2009; Barton et al. 2007; Fauque and Barton 2012) is consistent with our measurements.

198 It is common practice to normalize trace elements to P content, because P can be
199 measured simultaneously with trace elements by both ICP and SXRF methods, and can serve as
200 a proxy of cell biomass. However, the ~3-fold higher P content of *M. acetivorans* vs. *D.*
201 *multivorans* (Table 1) suggested that the elevated metal:P ratios in *D. multivorans* were driven
202 more by differences in P than in metal content. The higher P content of *M. acetivorans* may be
203 due to polyphosphate synthesis (Li et al. 2007).

204 *M. acetivorans* SXRF ratios for Fe:P, Co:P and Ni:P from the monoculture grown on
205 methanol are broadly consistent with those measured by ICP optical emission spectrometry for
206 six methanol-grown *Methanosarcina* species (37-171 Fe:P; 1-5 Co:P; 2-15 Ni:P mmol mol^{-1})
207 (Scherer et al. 1983). Lower Zn:P (2-21 mmol mol^{-1}) and Cu:P (0.3-1.0 mmol mol^{-1}) ratios
208 reported by Scherer et al. (1983) were likely due to the absence of those two metals from growth
209 media, whereas our medium contained 7 and 0.3 μM of Zn and Cu, respectively. Opposite trends
210 between *M. acetivorans* in this study (Co > Ni) and the six *M. acetivorans* species previously
211 analyzed (Ni > Co) were also likely due to differences in media composition: our medium
212 contained 2 μM Co and 0.9 μM Ni, whereas the Scherer et al. (1983) medium contained 5 μM Ni
213 and 1 μM Co. Higher metal:P ratios measured by ICP-MS than SXRF for cocultured cells may
214 be due to inclusion of metal-rich non-cellular particles in bulk ICP-MS analyses, which were
215 excluded in cell-targeted ROI analyses of SXRF maps. Indeed, ICP-MS Mn:P ratios for the
216 marine cyanobacterium *Trichodesmium* were consistently higher than SXRF measurements
217 (Nuester et al. 2012), suggesting that mineral particles that were excluded from single-cell SXRF
218 maps might have been included in bulk ICP-MS analyses.

Methanogenic archaea have been previously shown out-compete sulfate-reducing bacteria in the presence of methanol (Dawson et al. 2015), attributed to the slower growth rates of sulfate-reducing bacteria than methylotrophic methanogens at mesophilic temperatures (Weijma and Stams 2001), and supported by longer doubling times (99 h) for *D. multivorans* than *M. acetivorans* (38 h) grown on lactate or methanol, respectively (Dawson et al. 2015). Our SXRF maps showed that cells analyzed from the coculture (comprised of 77% *M. acetivorans*) contained 7 times higher P contents than *M. acetivorans* cells grown in monoculture. It is important to note that different sample preparation methods could have contributed to differing P content; cocultures were chemically fixed before SXRF analysis, whereas monocultures were not, and glutaraldehyde fixation has previously been found to increase the lability of internal P, leading to 50% lower cellular P content (Tang and Morel 2006). However, we observed *higher,* not lower, cellular P for chemically fixed cocultured cells. Instead, this elevated P might be indicative of increased polyphosphate production due to stress response in *M. acetivorans* (Li et al. 2007), possibly triggered by the presence of a potentially competing different species.

Turning to trace metals, our SXRF and ICP-MS data show that one (or both) of the species accumulated more cobalt when grown in coculture than monoculture. (SXRF data suggests that cellular Ni and Cu were also different in the mono- vs. cocultures, but since these trends were not consistent with ICP-MS data, we limit our discussion to cobalt.) This cellular cobalt enrichment in cocultures is unlikely to have originated from contamination by chemical fixation due the consistent trend in ICP-MS data of elevated cobalt in cocultures that were not subjected to chemical fixation, along with the unlikelihood that cobalt would have been the only contaminant present in trace metal-clean fixatives. Our medium contained 2 μM Co, within the optimal range for methylotrophic methanogens grown in monoculture (Jansen et al. 2007;

Scherer and Sahm 1981) and anaerobic digesters (Florencio et al. 1994; Florencio et al. 1993; Paulo et al. 2004). There are 18 genes encoding corrinoid-containing methyltransferases in *Methanosarcina acetivorans* and 6 genes encoding cobalt-containing proteins in *Desulfococcus oleovorans* (Zhang and Gladyshev 2010; Zhang et al. 2009). Cobalt is used in methanol:coenzyme M methyltransferase in the methanogen and corrinoid Fe-S methyltransferase protein in the Wood Ljungdahl pathway in both species (Ekstrom and Morel 2008; Fig. 4). Although the mechanism for cobalt enrichment remains unclear, our data suggest that the presence of a second microbial species in cocultures resulted in elevated cobalt uptake.

When grown at millimolar metal concentrations, sulfate-reducing bacteria efficiently remove metals from solution (Krumholz et al. 2003) and precipitate covellite (CuS; Gramp et al. 2006; Karnachuk et al. 2008), sphalerite (ZnS; Gramp et al. 2007), and pentlandite (Co_9S_8) (Sitte et al. 2013). The nanoparticulate zinc sulfide phase we imaged was likely sphalerite based on its ~1:1 Zn:S ratio, whereas the phase with the approximate stoichiometry $(CoCu)S_2$ may be mineralogically distinct from those produced at higher metal loadings. Our observation of two distinct classes of extracellular metal sulfide nanoparticles in microbial cocultures grown at environmentally relevant metal concentrations suggests that such nanoparticulate metal sulfides may occur in diverse anoxic settings, even those that are not contaminated with heavy metals. Moreover, our observation of higher than predicted Co:P and Cu:P ratios measured by ICP-MS for cocultures might be due to inclusion of nanoparticulate $(CoCu)S_2$ in these bulk analyses.

In sulfidic environments such as marine sediments and anaerobic digesters, dissolved Co and Ni concentrations are present in nanomolar concentrations (Glass et al. 2014; Jansen et al. 2005). These metals are predominantly present as solid metal sulfide precipitates and/or sorbed to anaerobic sludge (van Hullebusch et al. 2006; van Hullebusch et al. 2005; van Hullebusch et

al. 2004). The bioavailability of these solid phases to anaerobic microbes remains relatively unknown. Previous studies suggest that methanogenic archaea can leach Ni from silicate minerals (Hausrath et al. 2007) and metal sulfides (Gonzalez-Gil et al. 1999; Jansen et al. 2007). Sulfidic/methanogenic bioreactors (Jansen et al. 2005) and *D. multivorans* monocultures (Bridge et al. 1999) contain high-affinity Co-/Ni- and Cu-/Zn-binding ligands, respectively, which may aid in liberating metal micronutrients from solid phases when they become growth-limiting. Importantly, this study provides the first evidence that microbes have different metal quotas when grown in monoculture vs. coculture, and may precipitate different metal sulfide minerals when exposed to micromolar vs. millimolar metal concentrations.

Conclusions

Overall consistency between SXRF and bulk ICP-MS data suggests that the Bionanoprobe is a promising method for quantifying trace elements in anaerobic microbial cultures on a per-cell basis, as previously observed for other cell types (Fahrni 2007; Ingall et al. 2013; Kemner et al. 2004; Nuester et al. 2012; Twining et al. 2003; Twining et al. 2008). A benefit of SXRF imaging is elemental quantification of the specific cell of interest, whereas ICP-MS measurements cannot delineate the elemental contributions of co-occurring cell types. However, it was not possible to distinguish between methanogenic archaea and sulfate-reducing bacteria in coculture on the basis of cell morphology or elemental content, and attempts to image cells by fluorescence microscopy after SXRF analysis were unsuccessful due to x-ray radiation damage. Therefore, we recommend that future studies test the feasibility of FISH microscopy prior to SXRF analysis to correlate phylogenetic identity and elemental content.

Author Contributions

J.B.G., V.J.O., S.C., and K.S.D. conceived and designed the experiments; K.S.D. performed the microbial culturing, S.C., J.B.G., and S.V. performed the SXRF analyses; B.S.T. performed the ICP-MS analysis, J.B.G., S.C., D.R.H., S.V., E.D.I., and B.S.T. analyzed the data; and J.B.G. wrote the manuscript with input from all authors. All authors have given approval to the final version of the manuscript.

Funding Sources

This work was supported by a NASA Astrobiology Postdoctoral Fellowship to J.B.G, NASA Exobiology award NNX14AJ87G to J.B.G., DOE Biological and Environmental Research award DE-SC0004949 to V.J.O, and NSF award OCE-0939564 to V.J.O. Use of the Advanced Photon Source, an Office of Science User Facility operated for the U.S. DOE Office of Science by Argonne National Laboratory, was supported by the U.S. DOE under Contract No. DE-AC02-06CH11357. Use of the LS-CAT Sector 21 was supported by the Michigan Economic Development Corporation and the Michigan Technology Tri-Corridor (Grant 085P1000817).

Acknowledgements

We thank Shawn McGlynn for assistance with sample preparation, and Keith Brister, Junjing Deng, Barry Lai and Rachel Mak at LS-CAT for assistance with Bionanoprobe analysis. We thank Larry Barton and Joel Kostka for helpful discussions, and Marcus Bray, Amanda Cavazos, Grayson Chadwick, Chloe Stanton, and Nadia Szeinbaum for feedback on previous manuscript drafts.

308 **Table 1.** Mean and standard error (in parentheses) of cellular elemental contents measured by
309 SXRF. Monocultures were prepared without chemical fixation, and cocultures were prepared
310 with paraformaldehyde + glutaraldehyde fixation, followed by spotting onto silicon nitride
311 wafers as described in the text.

Culture	Substrate (mM)	Element per cell (mol x 10^{-18} $cell^{-1}$)						
		P	**S**	**Fe**	**Co**	**Ni**	**Cu**	**Zn**
100% *Methanosarcina acetivorans* DSM 2834 (n = 14)	Methanol (60 mM)	178 (28)	2167 (318)	19 (4)	1.5 (0.2)	0.20 (0.03)	4.9 (0.7)	17 (2)
100% *Desulfococcus multivorans* DSM 2059 (n = 18)	Lactate (20 mM)	59 (11)	111 (19)	26 (6)	0.6 (0.1)	0.13 (0.03)	3.7 (1.0)	46 (14)
77% *Methanosarcina acetivorans* DSM 2834, 23% *Desulfococcus multivorans* DSM 2059 (n = 13)	Methanol (60 mM), lactate (20 mM)	1252 (69)	855 (69)	13.0 (0.9)	7.2 (0.7)	1.5 (0.9)	0.5 (0.2)	8.5 (0.8)

312
313
314

315 **Table 2.** Phosphorus (P) normalized metal stoichiometries (mmol metal mol^{-1} P) of mono- and
316 cocultures measured by ICP-MS or SXRF. All values are measured except the last row, which
317 are predicted values for ICP-MS based on the relative abundance of the two species in coculture.
318 See text for discussion about differences between ICP-MS and SXRF results with P
319 normalization. Standard errors are in parentheses for SXRF data and analytical uncertainty is ±
320 5% for ICP-MS.

Culture	**Substrate (mM)**	**Technique**	**metal:P (mmol mol^{-1})**				
			Fe:P	**Co:P**	**Ni:P**	**Cu:P**	**Zn:P**
100% *Methanosarcina acetivorans* DSM 2834	Methanol (60 mM)	SXRF	105 (7)	8.4 (0.4)	1.18 (0.05)	28 (1)	104 (4)
		ICP-MS	26	16	5	3	43
100% *Desulfococcus multivorans* DSM 2059	Lactate (20 mM)	SXRF	508 (97)	11 (2)	2.5 (0.5)	80 (19)	930 (220)
		ICP-MS	184	99	22	16	235
77% *Methanosarcina acetivorans* DSM 2834, 23% *Desulfococcus multivorans* DSM 2059	Methanol (60 mM), lactate (20 mM)	SXRF	10.5 (0.5)	5.7 (0.4)	1.0 (0.6)	0.4 (0.1)	6.7 (0.4)
		ICP-MS	65	51	8	8	113
		ICP-MS (predicted)	81	45	12	7	111

321

Figure Captions

Figure 1. Box plot of cellular P, S, Fe, Co, Ni, Cu and Zn contents for monocultures of *Methanosarcina acetivorans* (white; n=14), monocultures of *Desulfococcus multivorans* (light grey; n=18), and cocultures of 77% *M. acetivorans* and 23% *D. multivorans* (dark grey; n=12) measured by SXRF. Different letters indicate statistically different elemental contents ($p < 0.05$ based on Tukey-Kramer HSD test).

Figure 2. SXRF co-localization of P (red), Co (green), and Zn (blue; left panel), and S (red), Ni (green), and Cu (blue; right panel) for whole cells of 77% *Methanosarcina acetivorans* and 23% *Desulfococcus multivorans* in coculture. Values in parentheses are maxima in μg cm^{-2} for each element.

Figure 3. SXRF co-localization of P (red), Co (green), and Zn (blue) in left panels, and S (red), Ni (green), and Cu (blue) in right panels for five imaged fields of 5 μm thin sections of 77% *Methanosarcina acetivorans* and 23% *Desulfococcus multivorans* cocultures. Values in parentheses are maxima in μg cm^{-2} for each element.

Figure 4. Schematic of metalloenzyme-containing metabolic pathways in the complete carbon-oxidizing sulfate-reducing bacterium *Desulfococcus mutitvorans* and the methylotrophic methanogenic archaeon *Methanosarcina acetivorans* as confirmed by genomic analyses, with interspecies H_2 transfer from methanol-fed *Methanosarcina* spp. to the sulfate-reducing bacterial species depicted as described by Phelps et al. (1985). Nickel (Acs, Cdh, Mcr) and cobalt (CFeSP, Mts, Mtr, and Sat) containing enzymes are labeled in bold. Enzyme abbreviations: Acs/CFeSP: acetyl-CoA synthase/corrinoid-FeS protein; Cdh: carbon monoxide dehydrogenase; Mts: methanol:coenzyme M methyltransferase; Mcr: methyl coenzyme M reductase; Mtr: methyl-tetrahydromethanopterin:coenzyme M methyltransferase; Sat: ATP sulfurylase.

References

Barton LL, Fauque GD. 2009. Biochemistry, physiology and biotechnology of sulfate□reducing bacteria. Adv Appl Microbiol 68:41-98.

Barton LL, Goulhen F, Bruschi M, Woodards NA, Plunkett RM, Rietmeijer FJM. 2007. The bacterial metallome: composition and stability with specific reference to the anaerobic bacterium *Desulfovibrio desulfuricans*. Biometals 20:291–302.

Berg IA. 2011. Ecological aspects of the distribution of different autotrophic CO2 fixation pathways. Appl Environ Microbiol 77(6):1925-1936.

Bridge TA, White C, Gadd GM. 1999. Extracellular metal-binding activity of the sulphate-reducing bacterium *Desulfococcus multivorans*. Microbiology 145(10):2987-2995.

Brileya KA, Camilleri LB, Zane GM, Wall JD, Fields MW. 2014. Biofilm growth mode promotes maximum carrying capacity and community stability during product inhibition syntrophy. Front Microbiol 5:693.

Bryant M, Campbell LL, Reddy C, Crabill M. 1977. Growth of *Desulfovibrio* in lactate or ethanol media low in sulfate in association with H2-utilizing methanogenic bacteria. Appl Environ Microbiol 33(5):1162-1169.

Cameron V, House CH, Brantley SL. 2012. A first analysis of metallome biosignatures of hyperthermophilic archaea. Archaea 2012:12.

Chen S, Deng J, Yuan Y, Flachenecker C, Mak R, Hornberger B, Jin Q, Shu D, Lai B, Maser J, Roehrig C, Paunesku T, Gleber SC, Vine DJ, Finney L, VonOsinski J, Bolbat M, Spink I, Chen Z, Steele J, Trapp D, Irwin J, Feser M, Snyder E, Brister K, Jacobsen C, Woloschak G, Vogt S. 2013. The Bionanoprobe: hard X-ray fluorescence nanoprobe with cryogenic capabilities. J Synchrotron Radiat 21(1):66-75.

Cvetkovic A, Menon AL, Thorgersen MP, Scott JW, Poole II FL, Jenney Jr FE, Lancaster WA, Praissman JL, Shanmukh S, Vaccaro BJ, Trauger SA, Kalisiak E, Apon JV, Siuzdak G, Yannone SM, Tainer JA, Adams MWW. 2010. Microbial metalloproteomes are largely uncharacterized. Nature 466:779-782.

Daims H, Stoecker K, Wagner M. 2005. Fluorescence in situ hybridization for the detection of prokaryotes. In: Osborn AM, Smith CJ, editors. Molecular Microbial Ecology. Abingdon, UK: Bios-Garland. p. 239.

Dawson K, Osburn M, Sessions A, Orphan V. 2015. Metabolic associations with archaea drive shifts in hydrogen isotope fractionation in sulfate□reducing bacterial lipids in cocultures and methane seeps. Geobiology 13(5):462-477.

Dawson KS, Strąpoć D, Huizinga B, Lidstrom U, Ashby M, Macalady JL. 2012. Quantitative fluorescence in situ hybridization analysis of microbial consortia from a biogenic gas field in Alaska's Cook Inlet Basin. Appl Environ Microbiol 78(10):3599-3605.

Demirel B, Scherer P. 2011. Trace element requirements of agricultural biogas digesters during biological conversion of renewable biomass to methane. Biomass Bioenerg. 35:992-998.

Ekstrom EB, Morel FMM. 2008. Cobalt limitation of growth and mercury methylation in sulfate-reducing bacteria. Environ Sci Tech 42(1):93-99.

Ermler U, Grabarse W, Shima S, Goubeaud M, Thauer RK. 1997. Crystal structure of methyl-coenzyme M reductase: the key enzyme of biological methane formation. Science 278(5342):1457-1462.

388 Fahrni CJ. 2007. Biological applications of X-ray fluorescence microscopy: exploring the
389 subcellular topography and speciation of transition metals. Curr Opin Chem Biol
390 11(2):121-127.
391 Fauque GD, Barton LL. 2012. Hemoproteins in dissimilatory sulfate- and sulfur-reducing
392 prokaryotes. Adv Microbiol Physiol 60:1-90.
393 Ferry JG. 2010. How to make a living by exhaling methane. Ann Rev Microbiol 64:453-473.
394 Finke N, Hoehler TM, Jørgensen BB. 2007. Hydrogen 'leakage'during methanogenesis from
395 methanol and methylamine: implications for anaerobic carbon degradation pathways in
396 aquatic sediments. Environ Microbiol 9(4):1060-1071.
397 Florencio L, Field JA, Lettinga G. 1994. Importance of cobalt for individual trophic groups in an
398 anaerobic methanol-degrading consortium. Appl Environ Microbiol 60(1):227-234.
399 Florencio L, Jenicek P, Field JA, Lettinga G. 1993. Effect of cobalt on the anaerobic degradation
400 of methanol. J Ferment Bioeng 75(5):368-374.
401 Gavel OY, Bursakov SA, Calvete JJ, George GN, Moura JJG, Moura I. 1998. ATP sulfurylases
402 from sulfate-reducing bacteria of the genus *Desulfovibrio*. A novel metalloprotein
403 containing cobalt and zinc. Biochem 37:16225-16232.
404 Gavel OY, Bursakov SA, Rocco GD, Trincao J, Pickering IJ, George GN, Calvete JJ, Shnyrov
405 VL, Brondino CD, Pereira AS. 2008. A new type of metal-binding site in cobalt-and
406 zinc-containing adenylate kinases isolated from sulfate-reducers *Desulfovibrio gigas* and
407 *Desulfovibrio desulfuricans* ATCC 27774. J Inorganic Biochem 102(5):1380-1395.
408 Glass JB, Orphan VJ. 2012. Trace metal requirements for microbial enzymes involved in the
409 production and consumption of methane and nitrous oxide. Front Microbiol 3:61.
410 Glass JB, Yu H, Steele JA, Dawson KS, Sun S, Chourey K, Pan C, Hettich RL, Orphan VJ.
411 2014. Geochemical, metagenomic and metaproteomic insights into trace metal utilization
412 by methane□oxidizing microbial consortia in sulphidic marine sediments. Environ
413 Microbiol 16(6):1592–1611.
414 Gonzalez-Gil G, Kleerebezem R, Lettinga G. 1999. Effects of nickel and cobalt on kinetics of
415 methanol conversion by methanogenic sludge as assessed by on-line CH4 monitoring.
416 Appl Environ Microbiol 65(4):1789–1793.
417 Gramp JP, Bigham JM, Sasaki K, Tuovinen OH. 2007. Formation of Ni-and Zn-sulfides in
418 cultures of sulfate-reducing bacteria. Geomicrobiol J 24(7-8):609-614.
419 Gramp JP, Sasaki K, Bigham JM, Karnachuk OV, Tuovinen OH. 2006. Formation of covellite
420 (CuS) under biological sulfate-reducing conditions. Geomicrobiol J 23(8):613-619.
421 Guss AM, Kulkarni G, Metcalf WW. 2009. Differences in hydrogenase gene expression between
422 *Methanosarcina acetivorans* and *Methanosarcina barkeri*. J Bacteriol 191(8):2826-2833.
423 Hagemeier CH, Kruer M, Thauer RK, Warkentin E, Ermler U. 2006. Insight into the mechanism
424 of biological methanol activation based on the crystal structure of the methanol-
425 cobalamin methyltransferase complex. Proc Natl Acad Sci 103(50):18917–18922.
426 Hamann N, Mander GJ, Shokes JE, Scott RA, Bennati M, Hedderich R. 2007. A cysteine-rich
427 CCG domain contains a novel [4Fe-4S] cluster binding motif as deduced from studies
428 with subunit B of heterodisulfide reductase from *Methanothermobacter marburgensis*.
429 Biochemistry 46(44):12875-12885.
430 Hausrath EM, Liermann LJ, House CH, Ferry JG, Brantley SL. 2007. The effect of methanogen
431 growth on mineral substrates: will Ni markers of methanogen based communities be
432 detectable in the rock record? Geobiology 5(1):49-61.

Ingall ED, Diaz JM, Longo AF, Oakes M, Finney L, Vogt S, Lai B, Yager PL, Twining BS, Brandes JA. 2013. Role of biogenic silica in the removal of iron from the Antarctic seas. Nature Comm 4:1981.

Jansen S, Gonzalez-Gil G, van Leeuwen HP. 2007. The impact of Co and Ni speciation on methanogenesis in sulfidic media—Biouptake versus metal dissolution. Enzyme Microb Tech 40:823-830.

Jansen S, Steffen F, Threels WF, Van Leeuwen HP. 2005. Speciation of Co (II) and Ni (II) in anaerobic bioreactors measured by competitive ligand exchange-adsorptive stripping voltammetry. Environ Sci Tech 39(24):9493-9499.

Karnachuk OV, Sasaki K, Gerasimchuk AL, Sukhanova O, Ivasenko DA, Kaksonen AH, Puhakka JA, Tuovinen OH. 2008. Precipitation of Cu-sulfides by copper-tolerant *Desulfovibrio* isolates. Geomicrobiol J 25(5):219-227.

Kemner KM, Kelly SD, Lai B, Maser J, O'loughlin EJ, Sholto-Douglas D, Cai Z, Schneegurt MA, Kulpa CF, Nealson KH. 2004. Elemental and redox analysis of single bacterial cells by X-ray microbeam analysis. Science 306(5696):686-687.

Krumholz LR, Elias DA, Suflita JM. 2003. Immobilization of cobalt by sulfate-reducing bacteria in subsurface sediments. Geomicrobiol J 20(1):61-72.

Li L, Li Q, Rohlin L, Kim U, Salmon K, Rejtar T, Gunsalus RP, Karger BL, Ferry JG. 2007. Quantitative proteomic and microarray analysis of the archaeon *Methanosarcina acetivorans* grown with acetate versus methanol. J Prot Res 6(2):759-771.

Loy A, Lehner A, Lee N, Adamczyk J, Meier H, Ernst J, Schleifer K-H, Wagner M. 2002. Oligonucleotide microarray for 16S rRNA gene-based detection of all recognized lineages of sulfate-reducing prokaryotes in the environment. Appl Environ Microbiol 68(10):5064-5081.

Macalady JL, Lyon EH, Koffman B, Albertson LK, Meyer K, Galdenzi S, Mariani S. 2006. Dominant microbial populations in limestone-corroding stream biofilms, Frasassi cave system, Italy. Appl Environ Microbiol 72(8):5596-5609.

McGlynn SE, Chadwick GL, Kempes CP, Orphan VJ. 2015. Single cell activity reveals direct electron transfer in methanotrophic consortia. Nature 526:531–535.

Neveu M, Poret□Peterson A, Anbar A, Elser J. 2016. Ordinary stoichiometry of extraordinary microorganisms. Geobiology 14(1):33-53.

Neveu M, Poret□Peterson AT, Lee ZM, Anbar AD, Elser JJ. 2014. Prokaryotic cells separated from sediments are suitable for elemental composition analysis. Limnol Oceangr: Methods 12(7):519-529.

Nuester J, Vogt S, Newville M, Kustka AB, Twining BS. 2012. The unique biochemical signature of the marine diazotroph *Trichodesmium*. Front Microbiol 3:1-15.

Oremland RS, Polcin S. 1982. Methanogenesis and sulfate reduction: competitive and noncompetitive substrates in estuarine sediments. Appl Environ Microbiol 44(6):1270-1276.

Osburn MR, Dawson KS, Fogel ML, Sessions AL. 2016. Fractionation of hydrogen isotopes by sulfate-and nitrate-reducing bacteria. Front Microbiol 7.

Outten CE, O'Halloran TV. 2001. Femtomolar sensitivity of metalloregulatory proteins controlling zinc homeostasis. Science 292(5526):2488-2492.

Ozuolmez D, Na H, Lever MA, Kjeldsen KU, Jørgensen BB, Plugge CM. 2015. Methanogenic archaea and sulfate reducing bacteria co-cultured on acetate: teamwork or coexistence? Front Microbiol 6:492.

Paulo LM, Stams AJ, Sousa DZ. 2015. Methanogens, sulphate and heavy metals: a complex system. Rev Environ Sci Biotech 14(4):537-553.

Paulo PL, Jiang B, Cysneiros D, Stams AJM, Lettinga G. 2004. Effect of cobalt on the anaerobic thermophilic conversion of methanol. Biotech Bioeng 85(4):434-441.

Pereira IAC, Ramos AR, Grein F, Marques MC, Da Silva SM, Venceslau SS. 2011. A comparative genomic analysis of energy metabolism in sulfate reducing bacteria and archaea. Front Microbiol 2(69):1-22.

Phelps T, Conrad R, Zeikus J. 1985. Sulfate-dependent interspecies H2 transfer between *Methanosarcina barkeri* and *Desulfovibrio vulgaris* during coculture metabolism of acetate or methanol. Appl Environ Microbiol 50(3):589-594.

Price NM, Harrison GI, Hering JG, Hudson RJ, Nirel PM, Palenik B, Morel FM. 1988. Preparation and chemistry of the artificial algal culture medium Aquil. Biol Oceanogr 6(5-6):443-461.

Ragsdale SW, Kumar M. 1996. Nickel-containing carbon monoxide dehydrogenase/acetyl-CoA synthase. Chem Rev 96(7):2515-2540.

Raskin L, Poulsen LK, Noguera DR, Rittmann BE, Stahl DA. 1994. Quantification of methanogenic groups in anaerobic biological reactors by oligonucleotide probe hybridization. Appl Environ Microbiol 60(4):1241-1248.

Rouf M. 1964. Spectrochemical analysis of inorganic elements in bacteria. J Bacteriol 88(6):1545-1549.

Scherer P, Lippert H, Wolff G. 1983. Composition of the major elements and trace elements of 10 methanogenic bacteria determined by inductively coupled plasma emission spectrometry. Biol Trace Elem Res 5(3):149-163.

Scherer P, Sahm H. 1981. Effect of trace elements and vitamins on the growth of *Methanosarcina barkeri*. Acta Biotechnol 1(1):57-65.

Sitte J, Pollok K, Langenhorst F, Küsel K. 2013. Nanocrystalline nickel and cobalt sulfides formed by a heavy metal-tolerant, sulfate-reducing enrichment culture. Geomicrobiol J 30(1):36-47.

Spanjers H, Weijma J, Abusam A. 2002. Modelling the competition between sulphate reducers and methanogens in a thermophilic methanol-fed bioreactor. Water Sci Tech 45(10):93-98.

Stams AJ, Plugge CM. 2009. Electron transfer in syntrophic communities of anaerobic bacteria and archaea. Nat Rev Microbiol 7(8):568-577.

Tang D, Morel FMM. 2006. Distinguishing between cellular and Fe-oxide-associated trace elements in phytoplankton. Mar Chem 98:18-30.

Thauer RK, Kaster A-K, Goenrich M, Schick M, Hiromoto T, Shima S. 2010. Hydrogenases from methanogenic archaea, nickel, a novel cofactor, and H2 storage. Ann Rev Biochem 79:507-536.

Thauer RK, Kaster A-K, Seedorf H, Buckel W, Hedderich R. 2008. Methanogenic archaea: ecologically relevant differences in energy conservation. Nat Rev Microbiol 6:579-591.

Twining BS, Baines SB, Fisher NS, Maser J, Vogt S, Jacobsen C, Tovar-Sanchez A, Sanudo-Wilhelmy SA. 2003. Quantifying trace elements in individual aquatic protist cells with a synchrotron X-ray fluorescence microprobe. Anal Chem 75(15):3806-3816.

Twining BS, Baines SB, Vogt S, de Jonge MD. 2008. Exploring ocean biogeochemistry by single-cell microprobe analysis of protist elemental composition. J Eukaryot Microbiol 55(3):151-162.

van Hullebusch ED, Gieteling J, Zhang M, Zandvoort MH, Daele WV, Defrancq J, Lens PNL. 2006. Cobalt sorption onto anaerobic granular sludge: Isotherm and spatial localization analysis. J Biotechnol 121(2):227-240.

van Hullebusch ED, Peerbolte A, Zandvoort MH, Lens PNL. 2005. Sorption of cobalt and nickel on anaerobic granular sludges: isotherms and sequential extraction. Chemosphere 58(4):493-505.

van Hullebusch ED, Zandvoort MH, Lens PNL. 2004. Nickel and cobalt sorption on anaerobic granular sludges: kinetic and equilibrium studies. J Chem Tech Biotech 79(11):1219-1227.

Vogt S. 2003. MAPS: A set of software tools for analysis and visualization of 3D X-ray fluorescence data sets. J Phys IV 104:635-638.

Weijma J, Stams A. 2001. Methanol conversion in high-rate anaerobic reactors. Water Sci Tech 44(8):7-14.

Zandvoort MH, Geerts R, Lettinga G, Lens PNL. 2003. Methanol degradation in granular sludge reactors at sub-optimal metal concentrations: role of iron, nickel and cobalt. Enzyme Microbiol Tech 33(2-3):190-198.

Zandvoort MH, van Hullebusch ED, Gieteling J, Lens PNL. 2006. Granular sludge in full-scale anaerobic bioreactors: trace element content and deficiencies. Enzyme Microbiol Tech 39(2):337-346.

Zhang Y, Gladyshev VN. 2010. dbTEU: a protein database of trace element utilization. Bioinformatics 26(5):700-702.

Zhang Y, Rodionov DA, Gelfand MS, Gladyshev VN. 2009. Comparative genomic analyses of nickel, cobalt and vitamin B12 utilization. BMC Genomics 10(78):1-26.

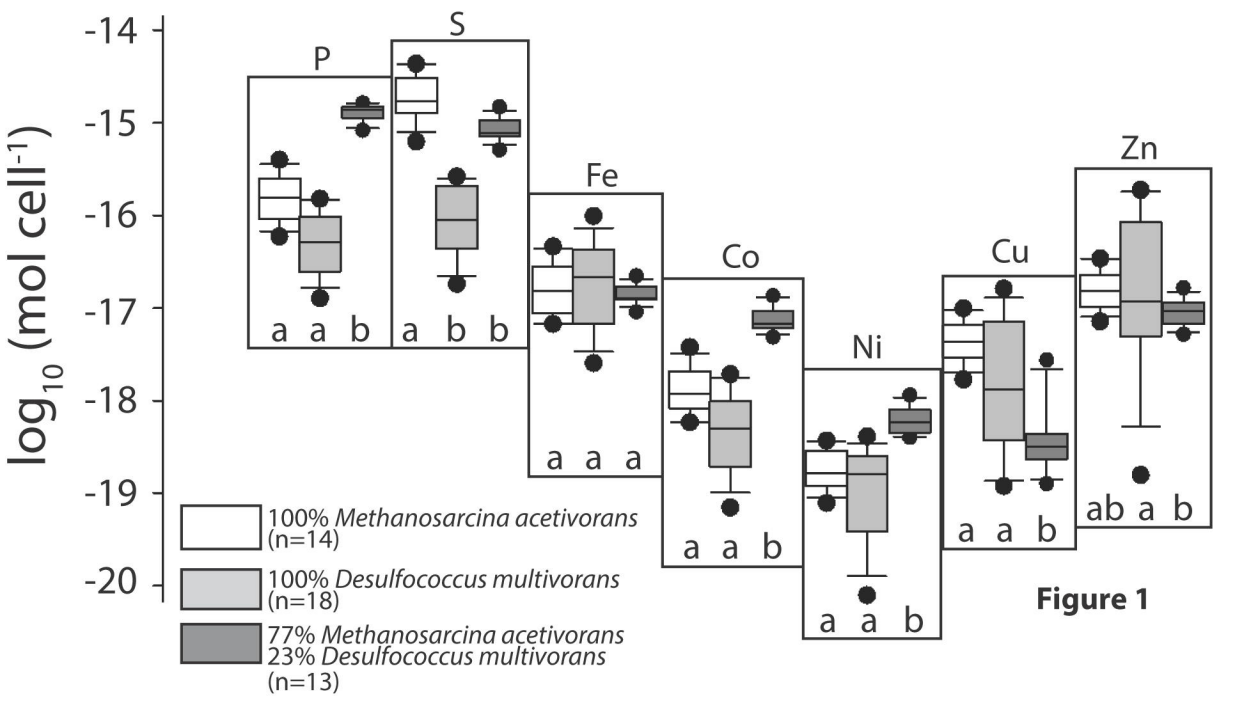
log10 (mol cell-1)
-14
-15
-16
-17
-18
-19
-20
P
S
Fe
Co
Ni
Cu
Zn
a a b
a b b
a a a
a a b
a a b
a a b
ab a b
100% Methanosarcina acetivorans (n=14)
100% Desulfococcus multivorans (n=18)
77% Methanosarcina acetivorans 23% Desulfococcus multivorans (n=13)

Figure 1

10 μm

Figure 2

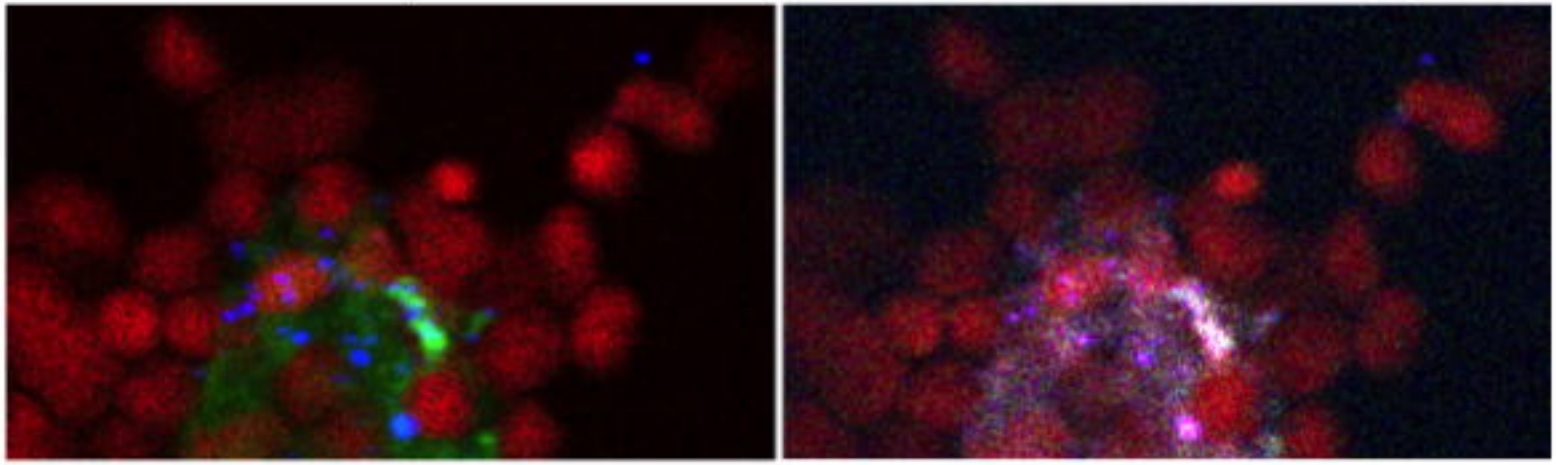

P (3.5) Co (0.4) Zn (0.7)

S (2.7) Ni (0.03) Cu (0.04)

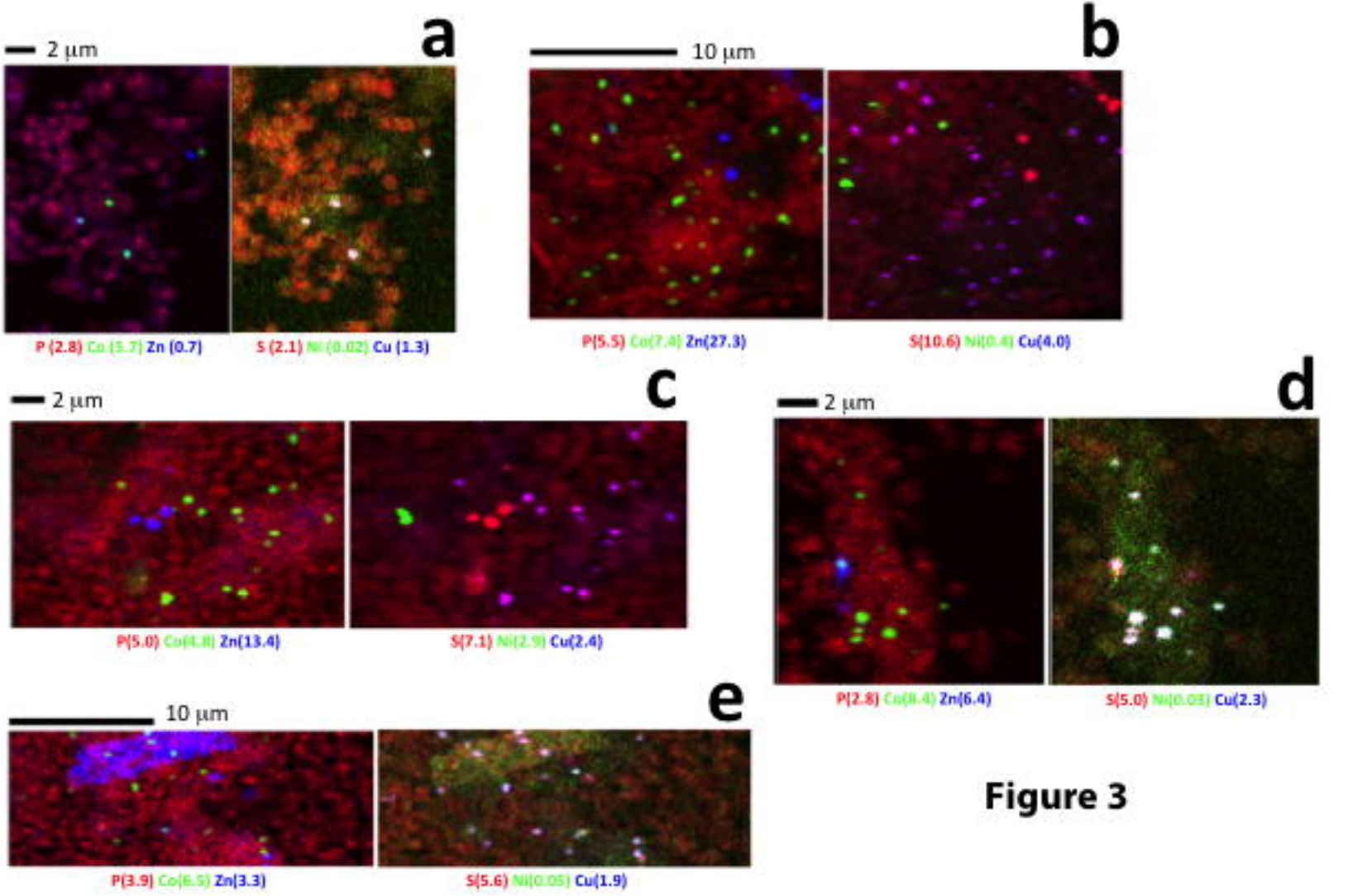
a
2 μm
P (2.8) Co (5.7) Zn (0.7)
S (2.1) Ni (0.02) Cu (1.3)
b
10 μm
P(5.5) Co(7.4) Zn(27.3)
S(10.6) Ni(0.4) Cu(4.0)
c
2 μm
P(5.0) Co(4.8) Zn(13.4)
S(7.1) Ni(2.9) Cu(2.4)
d
2 μm
P(2.8) Co(8.4) Zn(6.4)
S(5.0) Ni(0.03) Cu(2.3)
e
10 μm
P(3.9) Co(6.5) Zn(3.3)
S(5.6) Ni(0.05) Cu(1.9)

Figure 3

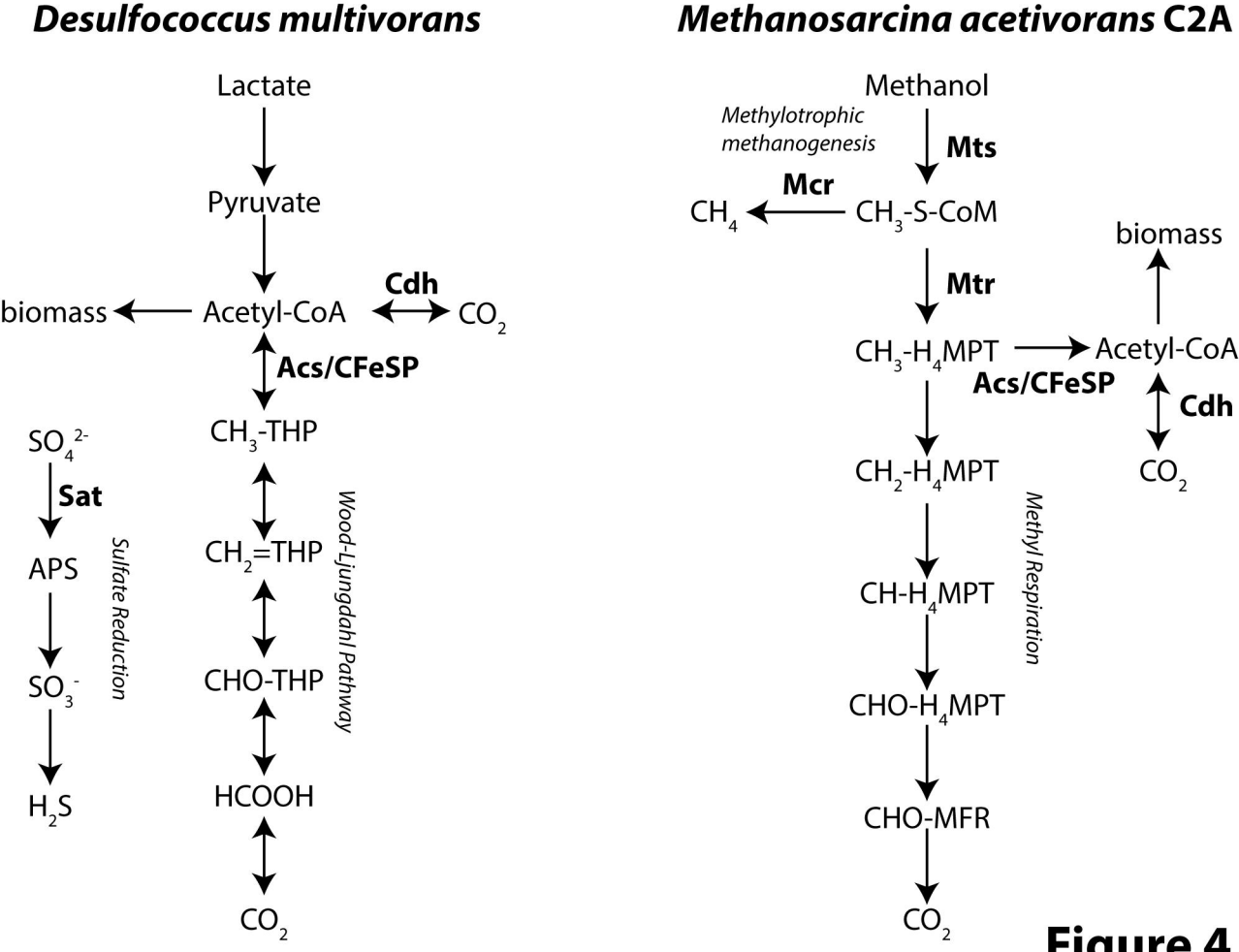
Desulfococcus multivorans
Lactate
Pyruvate
biomass
Acetyl-CoA
Cdh
CO2
Acs/CFeSP
CH3-THP
SO4 2-
Sat
APS
SO3 -
H2S
Sulfate Reduction
CH2=THP
CHO-THP
HCOOH
CO2
Wood-Ljungdahl Pathway
Methanosarcina acetivorans C2A
Methanol
Methylotrophic methanogenesis
Mts
Mcr
CH4
CH3-S-CoM
Mtr
CH3-H4MPT
Acetyl-CoA
Acs/CFeSP
Cdh
biomass
CO2
CH2-H4MPT
CH-H4MPT
CHO-H4MPT
CHO-MFR
CO2
Methyl Respiration

Figure 4